2nd URSI AT-RASC, Gran Canaria, 28 May – 1 June 2018

Magnet-free non-reciprocal photonic platform based on time-modulated graphene

D. Correas-Serrano and J. S. Gomez-Diaz*
Department of Electrical and Computer Engineering, University of California Davis
One Shields Avenue, Kemper Hall 2039, Davis, CA 95616, USA. *E-mail: jsgomez@ucdavis.edu

Abstract - *We propose a novel paradigm to achieve giant photonic non-reciprocity based on time-modulated graphene capacitors coupled to photonic waveguides, without reliance on any magneto-optic effects. The resulting hybrid graphene-dielectric platform is low-loss, silicon-compatible, robust against graphene's imperfections, scalable from terahertz to near infrared frequencies, and it exhibits very large nonreciprocal responses using realistic biasing schemes. Analytical frameworks based on solving the eigenstates of the modulated structure and on spatial coupled mode theory have been developed to unveil the underlying physics that dominate the proposed platform and to quickly design and analyze various isolators. Results, validated through harmonic balance full-wave simulations, confirm the flexibility of our low-loss (<3dB) platform to engineer a wide variety of responses and even to extend the isolation bandwidth. We envision that this technology will pave the wave to magnetic-free, fully-integrated, and CMOS-compatible nonreciprocal components with wide applications in sensing, communication systems, and optical networks.*

1. Introduction

Lorentz reciprocity requires that the response of a device is unchanged when excitation and observation points are swapped [1]. This fundamental property limits how signals are processed and transmitted on most linear devices. Non-reciprocal systems, which are not bounded by this symmetry, have become of critical importance throughout the entire frequency spectrum in the form of devices like circulators and isolators [2], [3], as they are required for full-duplex communications, radar operation, and to protect sensitive laser sources from unwanted reflections.

Non-reciprocity has traditionally been achieved almost exclusively through magneto-optical effects [2], [4]. This approach requires lossy and bulky magnetic materials under strong biasing fields, making it incompatible with modern technology trends that constantly pursue miniaturized, integrated, and affordable devices. Motivated by these shortcomings, recent years have seen a rapidly growing interest on alternative ways to break reciprocity, mainly through nonlinear materials [5] and spatiotemporal modulations able to impart linear or angular momentum to the waves propagation within the system [4]. Even though

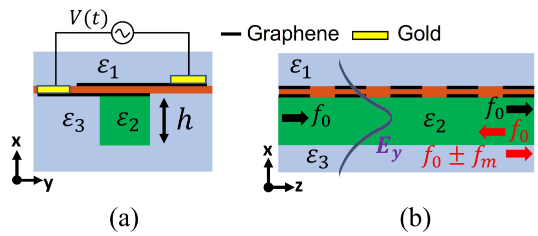

Figure 1. (a) Dielectric waveguide loaded with a time-modulated graphene capacitor. (b) Concept of a photonic isolator based on a slab waveguide coupled with spatiotemporally modulated graphene. When excited from the left at frequency f_0, all power is transmitted. When excited from the right, it is frequency-converted to $f_0 \pm f_m$ and reflected.

the former method does not require an external bias, it is limited to high intensity signals and excitation from a single port at a time. The latter approach is intensity-independent and provides greater design flexibility, which has allowed researchers to put forward a wide variety of magnet-less non-reciprocal devices in electromagnetics and acoustics [4]. Unfortunately, the use of these approaches in practical applications beyond RF remains very challenging due to the high modulation frequencies required –not achievable with commercial switches or varactors– and the difficulty of modulating the permittivity of silicon, typically done with highly lossy PIN junctions [6].

Here we propose to break reciprocity by using spatiotemporally modulated graphene as a *perturbation* of high-Q photonic modes in dielectric structures. The resulting hybrid graphene-dielectric photonic devices are low-loss, silicon-compatible, frequency-scalable, robust against graphene's imperfections, and exhibit large non-reciprocal responses using a realistic biasing scheme. We emphasize the intrinsic compatibility of this platform with well-established integrated photonic systems, as graphene is used *only* to engineer the required non-reciprocal coupling between photonic states, having negligible effect on their impedance, wavenumber, and modal profile. This contrasts with plasmonic devices based on 2D materials, which present exciting miniaturization and reconfiguration capabilities but typically introduce high loss [7], [8]. We illustrate the capabilities and broad reach of this novel platform by designing and analyzing different types of isolators based on linear and angular momentum, achieving low-loss (<3 dB) and high isolation (>35 dB) on a narrowband and even good isolation over a large bandwidth (15%). To this purpose, analytical frameworks based on solving the eigenstates of the modulated structure and on spatial coupled mode theory have been derived. Results, validated with full-wave simulations, confirm the exciting response of the proposed platform, significantly outperforming alternative approaches in this frequency band, while keeping full compatibility with CMOS technology and integrated circuits [9].

2. Isolators based on modulated graphene

Let us consider the structure of Fig. 1a, where a pair of closely spaced graphene sheets have been deposited in the vicinity of a dielectric waveguide with core permittivity ε_2 surrounded by media ε_1 and ε_3. For deeply subwavelength separation, which is desired in practice, the graphene stack has an effective conductivity that is the sum of the two layers, $\sigma_{stack} \approx \sigma_1 + \sigma_2$ and can be modulated by applying a voltage between them, enabling broad control of the stack conductivity [10]. If multiple of these capacitors are placed along the propagation direction z of a waveguide, as shown in Fig. 1b, one can find through standard techniques the voltages required in each capacitor to approximately yield an effective spatially and temporarily varying conductivity profile of the form [10]–[14]

$$\sigma_{eff}(z,t) = \sigma_{stack}\big(1 + M \cdot \cos(\omega_m t - k_m z)\big) \qquad (1)$$

where M is the modulation depth, t is time, ω_m is the modulation frequency, and $k_m = 2\pi/p$ is the modulation wavenumber, being p the spatial periodicity. This effective conductivity can be exploited to implement various types of photonic isolators by imparting linear able to induce asymmetric bandgaps and photonic interband transitions. At the conference we will also discuss realizations based on angular momentum and resonant elements, which allows to reduce the device footprint but sacrifices bandwidth.

We begin by focusing on a simple isolator based on asymmetric bandgaps for the fundamental TE mode of the dielectric waveguide in Fig. 1. It is well known that any periodic perturbation to a waveguide can be used to engineer photonic bandgaps, in which the propagation constant acquires an imaginary part that represents decay due to back-scattering [4]. This is the operation principle of Bragg gratings. The isolator proposed here is based on a similar principle, but with a major difference: the time-varying nature of the perturbation frequency-shifts the bandgaps in opposite directions for left-right and right-left propagation. This is analogous to the Doppler effect that would be observed if a Bragg grating was physically moving along the z-axis [15]. To analyze the response of this system, we rigorously find the eigenstates of the modulated waveguide by decomposing the fields in an infinite summation of spatial and frequency harmonics,

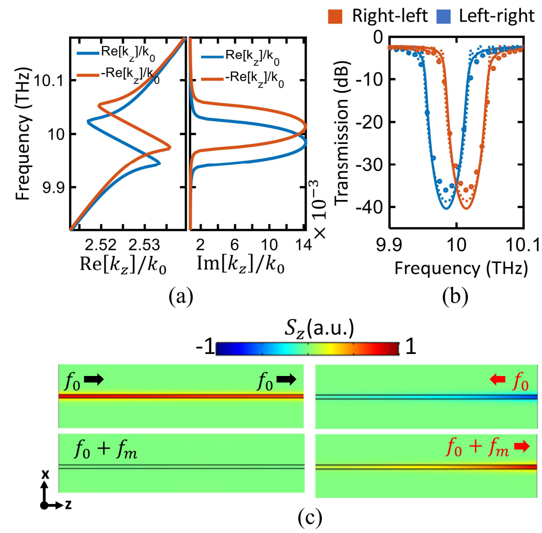

Figure 2. (a) Real and imaginary part of the wavenumber of the fundamental harmonic in isolator of Fig. 1, near the bandgap. Results have been computed analytically for both propagation directions. (b) Bidirectional transmission, computed with three different approaches: (i) considering the propagation decay given by the bandgaps given from Eq. (3) (solid lines), (ii) applying coupled mode theory with the dispersion and field profiles of the unmodulated waveguide (dotted lines); and (iii) using harmonic balance full-wave simulation in COMSOL Multiphysics (markers). Graphene's chemical potential and relaxation time are 0.4 eV and 1.0 ps, respectively, modulation frequency is 30 GHz, modulation index is 0.3, and temperature is 300 K.

allowing us to accurately compute the attenuation at the bandgaps, which in turn permits to calculate the reflectivity for a given waveguide length. Mathematical details are omitted here for the sake concreteness. The resulting dispersion relation takes the form of an infinite set of equations as

$$\frac{A_i}{\omega_i \mu_0}\left(-k_{yi} \; + jc_b k_{yi}\right) = \sigma_{\text{stack}}\left(A_i + \frac{A_{i+1}M}{2} + \frac{A_{i-1}M}{2}\right), \quad (2)$$

where μ_0 is the free-space permeability, i is the Floquet harmonic number, and c_b and A are amplitude constants. This set of equations can be truncated to a few terms in order to solve the determinantal equation for $k_{yi} = \sqrt{\varepsilon_r k_0^2 - k_{zi}^2}$, i.e., the y-component of the wavevector in the medium n for the ith spatiotemporal harmonic. The rest of harmonics have a wavenumber and frequency $k_{zi} \pm n k_m$, $\omega \pm n\omega_m$. Fig 2a shows the real and imaginary part of the fundamental harmonic's wavenumber near the bandgap for such a waveguide, with the values for left-right and right-left propagation plotted along the same axis for easier visualization. If the excitation frequency lies within a range where only positive or negative k_z have a large imaginary part, arbitrarily large isolation can be achieved as waves will be reflected in that direction, but not in the opposite one. Fig. 2b shows the transmission through the waveguide when it is excited from the left and the right, computed using three different approaches: (i) considering the propagation decay given by the bandgaps given from Eq. (3), (ii) applying coupled mode theory [3], [16] with the dispersion and field profiles of the unmodulated waveguide; and (iii) using harmonic balance full-wave simulation in COMSOL Multiphysics, all three showing excellent agreement. Fig. 2c shows the *z*-component of the Poynting vector for excitation from both sides at 10.01 THz, clearly illustrating the operation principle predicted by the asymmetric bandgap. Importantly, the reflected wave in the isolated direction is frequency-converted to $f_0 + f_m$ –note that the structure could be designed to instead couple to $f_0 - f_m$ by simply reversing the effective velocity of the modulation, i.e. changing the sign of k_m. Further details on the coupled mode theory approach, which is also fully analytical and allows to analyze a greater variety of isolators, will be provided at the conference. It is based on general coupled mode equations in space combined with the novel case of a modulated graphene stack. Within this framework, the isolator proposed above can also be understood as mediated by non-reciprocal coupling of modes propagating in opposite directions, and the response accurately predicted from the (much simpler) description of the system in the absence of any modulation.

At the conference, we will discuss the possibility of reducing the footprint of this type of isolators by using a resonant, spatiotemporally modulated, ring coupled to an unmodulated bus waveguide, achieving a greater than 10-fold reduction in device length. All mode coupling and frequency conversion now takes place within the ring, forming a resonant state that is a hybridization of the forward and frequency-converted backward [4], [17], [18]. In addition, we will also present at the conference a different approach to realize magnet-free isolators by using spatiotemporal modulation to couple otherwise orthogonal modes in a multimode structure, so that in the isolated direction all power is converted to the orthogonal mode which then can be filtered or scattered [11], [17]. In the connected direction, phase matching does not hold and thus no conversion occurs. This mode conversion is an 'interband photonic transition', in analogy with electron transitions between bands in semiconductors. We will detail various implementations at the conference, including theoretical and numerical results with realistic parameters. The differences between the various types of isolators based on this novel modulation scheme will be unveiled, including trade-offs in terms of loss, isolation, bandwidth, and potential ease of implementation.

Although we have limited our analysis in this paper to isolators, the versatility and far-reaching implications of the proposed platform should be emphasized: it can be employed to develop low-loss photonic circulators, Faraday rotators, as well as to manipulate nonreciprocity at the micro/nano scale to realize advanced functionalities such as nonreciprocal beam-steering and lensing, among many others. More importantly, this technology overcomes most of the challenges of the state of the art in terms of CMOS-compatibility and integration, miniaturization, losses, and performance. We envision that this paradigm will lead to a new generation of nonreciprocal photonic components with wide implications in sensing, antennas and communication systems, and optical networks.

3. References

1. H. B. G. Casimir, "On Onsager's principle of microscopic reversibility," *Rev. Mod. Phys.*, vol. 17, no. 2–3, pp. 343–350, Apr. 1945.

2. R. E. Collin, *Foundations for microwave engineering*. John Wiley & Sons, 2007.

3. A. Yariv and P. Yeh, *Optical waves in crystals*, vol. 10. Wiley, New York, 1984.

4. D. L. Sounas and A. Alù, "Non-reciprocal photonics based on time modulation," *Nat. Photonics*, vol. 11, no. 12, pp. 774–783, 2017.

5. D. L. Sounas and A. Alù, "Time-Reversal Symmetry Bounds on the Electromagnetic Response of Asymmetric Structures," *Phys. Rev. Lett.*, vol. 118, no. 15, p. 154302, 2017.

6. H. Lira, Z. Yu, S. Fan, and M. Lipson, "Electrically driven nonreciprocity induced by interband photonic transition on a silicon chip," *Phys. Rev. Lett.*, vol. 109, no. 3, pp. 1–5, 2012.

7. H. Buljan, M. Jablan, and M. Soljačić, "Graphene plasmonics: Damping of plasmons in graphene," *Nat. Photonics*, vol. 7, no. 5, pp. 346–348, 2013.

8. D. Correas-Serrano, A. Alù, and J. S. Gomez-Diaz, "Plasmon canalization and tunneling over anisotropic metasurfaces," *Phys. Rev. B*, 2017.

9. M. Tamagnone *et al.*, "Near optimal graphene terahertz non-reciprocal isolator," *Nat. Commun.*, vol. 7, pp. 1–6, 2016.

10. J. S. Gomez-Diaz *et al.*, "Self-biased reconfigurable graphene stacks for terahertz plasmonics," *Nat. Commun.*, vol. 6, no. 6334, pp. 1–8, May 2015.

11. D. Correas-Serrano, J. S. Gomez-Diaz, D. L. Sounas, Y. Hadad, A. Alvarez-Melcon, and A. Alu, "Nonreciprocal Graphene Devices and Antennas Based on Spatiotemporal Modulation," *IEEE Antennas Wirel. Propag. Lett.*, vol. 15, no. c, pp. 1529–1533, 2016.

12. D. Correas-Serrano, J. S. Gomez-Diaz, D. L. Sounas, A. Alvarez-Melcon, and A. Alù, "Non-reciprocal THz components based on spatiotemporally modulated graphene," in *2016 10th European Conference on Antennas and Propagation (EuCAP)*, 2016, pp. 1–4.

13. C. T. Phare, Y.-H. Daniel Lee, J. Cardenas, and M.

Lipson, “Graphene electro-optic modulator with 30 GHz bandwidth,” *Nat. Photonics*, vol. 9, no. 8, pp. 511–514, 2015.

14. D. Correas-Serrano, J. S. Gomez-Diaz, J. Perruisseau-Carrier, and A. Alvarez-Melcon, “Graphene-based plasmonic tunable low-pass filters in the terahertz band,” *IEEE Trans. Nanotechnol.*, vol. 13, no. 6, 2014.

15. N. Chamanara, S. Taravati, and C. Caloz, “Optical Isolation based on Space-time Engineered Asymmetric Photonic Bandgaps,” 2017.

16. H. Haus, *Waves and Fields in Optoelectronics*, vol. 32, no. 7. 1985.

17. Z. Yu and S. Fan, “Complete optical isolation created by indirect interband photonic transitions,” *Nat. Photonics*, vol. 3, no. 2, pp. 91–94, Jan. 2009.

18. R. Fleury, D. L. Sounas, C. F. Sieck, M. R. Haberman, and A. Alu, “Sound isolation and giant linear nonreciprocity in a compact acoustic circulator.,” *Science*, vol. 343, no. 6170, pp. 516–9, Jan. 2014.